JOURNAL OF AIRCRAFT
Vol. 43, No. 4, July–August 2006

Aerodynamics of Formation Flight

Z. A. Bangash,* R. P. Sanchez,* and A. Ahmed†
Auburn University, Alabama 36849
and
M. J. Khan‡
Tuskegee University, Alabama 36088

Reported are the results of wind-tunnel tests conducted to evaluate aerodynamics characteristics of aircraft in formation flight. A vortex-lattice numerical scheme was used to investigate the effect of spatial offset (horizontal and vertical) between the leading and trailing wings. The wind-tunnel test configurations consisted of echelon, chevron, and in-line formations. Analysis of the data revealed that the spatial offset and the angle of attack of the leading wing had significant impact on the trailing aircraft. For some test conditions an increase in lift-to-drag ratio of the trailing aircraft was measured. Variation in C_{Lmax} and/or α_{stall} was observed as well. At higher angles of attack of the leading wing, the C_L-α curve of the trailing aircraft was significantly altered.

Nomenclature

b	=	span, in.
b'	=	vortex span (distance between centroids of vortices)
C	=	rolling-moment coefficient
C_D	=	total drag coefficient
C_L	=	total lift coefficient
$C_{L\alpha}$	=	lift-curve slope, deg
c	=	cord length, in.
D	=	drag, lb
ds	=	length of vortex segment, in.
dy	=	normalized overlap distance between wing tips of leading aircraft and trailing aircraft
L	=	lift, lb
r	=	radial distance from vortex core, in.
t	=	time, s
V	=	freestream velocity, ft/s
W	=	upwash
x, y, z	=	coordinate system, origin at trailing aircraft wing quarter-chord
α	=	angle of attack, deg
Γ	=	circulation, ft^2/s
Δ	=	change
ε	=	downwash angle, deg
ν	=	kinematic viscosity

Subscripts

f	=	in formation
lw	=	leading wing
tw	=	trailing wing
x, y, z	=	components in x, y, z direction

Presented as Paper 2004-725 at the AIAA 42nd Aerospace Sciences Meeting and Exhibit, Reno, NV, 5–8 January 2004; received 8 October 2004; revision received 16 March 2005; accepted for publication 17 March 2005.

*Graduate Research Assistant, Department of Aerospace Engineering. Student Member AIAA.
†Associate Professor, Department of Aerospace Engineering. Associate Fellow AIAA.
‡Associate Professor, Aerospace Science Engineering Department. Senior Member AIAA.

Introduction

THE drag characteristics at higher C_L, as well as the adverse effects of wing-tip vortices, have been documented earlier.[1] A small decrease in induced drag can result in significant fuel savings over long-range flights. Although high-aspect-ratio wings have higher aerodynamic efficiency, large wing-root bending moments impose a prohibitive structural weight penalty because of strength requirments. Observation of close-formation flight of migratory birds has therefore motivated aerospace engineers to look closely at similar flight configurations of multiple aircraft for possible energy savings.[2]

Relative position of aircraft in formation flight is of critical importance as downwash and trailing vortices of the leading aircraft can result in imbalanced roll[1,3,4] in the trailing aircraft. Similar flight scenarios have been therefore investigated for optimizing performance.[5,6]

The mechanism of lift production in the case of birds is the result of flapping wings, which form a closed-loop vortex with wavy vortex lines at the wing tip and spanwise waves generated at every feather tip. During downstroke, the wing produces lift, and thrust is generated as a result of forward pivoting of the wing about its axis. During upstroke, the wing flexes in towards the body (largely because of a rotation of the humerus about its long axis) and then rises and extends for the next downstroke. Passive aerodynamic lift provides the restoring force for the upstroke under most cruising conditions.[7]

The aerodynamic advantage of the formation flight of birds is mainly based on the downwash generated by the leading bird and the resulting upwash and wing-tip vortex, which the trailing bird "rides."[8] The feather tips form a number of streamwise vortices along the span, which results in a high energy flow for the trailing bird. The combination of these two factors results in increased lift but with a small increase in overall drag as a result of a higher effective angle of attack.[9]

The bird leading the flock thus generates temporally and spatially varying flow conditions for the trailing bird in formation flight. However flow in the wake of fixed-wing flight vehicles is characterized by a continuous sheet of vorticity as opposed to discrete and/or periodic shedding of vortices from flapping wings. The presence of a well-defined trailing vortex and regions of upwash and downwash along with continuous circulation of the leading aircraft causes a temporally uniform but spatially varying flow condition for the trailing aircraft. The interference factors can thus include variation in C_{Lmax} or α_{stall}, spanwise flow on the surface of the trailing wing, cancellation or merging of the wing-tip vortices, and variation in effective angle of attack.[6]

An experimental investigation was therefore conducted to determine the dominant features of vortex interaction and subsequent

variations in aerodynamic forces of a model aircraft subjected to parametric changes in upstream conditions similar to those encountered in a variety of formation-flight configurations.

Vortex-Lattice Model

The leading aircraft wing was modeled using lifting-line theory, idealizing the wing as a bound vortex, and the wake was simulated as trailing vortices of the same strength as the bound vortex, thus making a horseshoe pattern. The strength of bound vortex was obtained from Kutta–Jukowski theorem, in terms of lift/unit span, the circulation of which is given by

$$\Gamma = L/\rho V b' \tag{1}$$

The vortex span b' was assumed to be equal to the wing span b. The trailing wing was modeled with a MATLAB®-based vortex-lattice code using 400 control points. The three primary parameters that could be varied included the dy and z location of semi-infinite vortex and circulation. The influence of the trailing vortices from the leading wing on the flowfield of the trailing wing was calculated by using the Biot–Savart law. The circulation of the wing-tip vortex is given by

$$\Gamma = \Gamma_o\left(1 - e^{-r^2/\nu t}\right) \tag{2}$$

where the time of travel t for the vortex from leading wing tip to impinging on trailing wing was calculated for 200-fps wind speed. The velocity thus induced by the wing-tip vortex is given by

$$V_{z(y)} = \frac{\Gamma}{2\pi}\int \frac{\boldsymbol{ds} \times \boldsymbol{r}}{r^3} \tag{3}$$

The results, with a Lamb–Oscene core, closely match the conventional profile of wing-tip vortex.[10] The coordinate system used for numerical calculations is depicted in Fig. 1.

The local upwash angle was calculated, and the average value of $\Delta\alpha$ was determined over the span of the trailing aircraft wing. The results of these calculations are listed in Table 1.

Table 1 Average Γ for half-span for various cases

α_{lw}	C_{Llw}	L_{lw}, lb	Γ, ft²/s	$\Delta\alpha$, deg
0	0	0	0	0
2	0.1556	3.91	14.31	0.76
4	0.3112	7.82	28.63	1.51
6	0.4668	11.73	42.94	2.26
8	0.6224	15.65	57.28	3.01
10	0.778	19.57	71.59	3.76

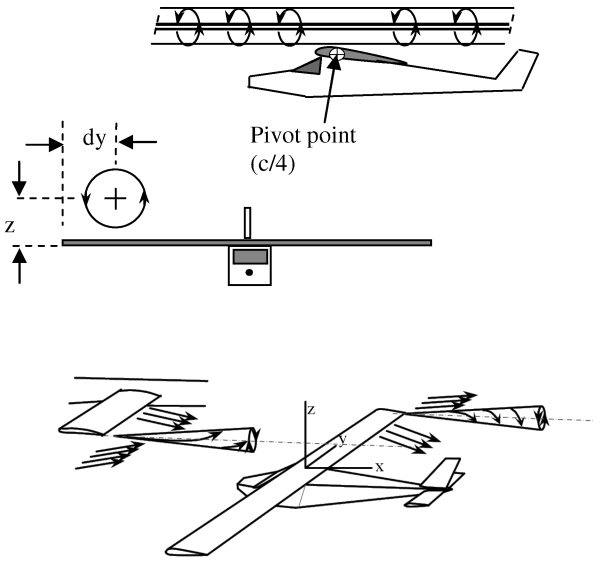

Fig. 1 Simplified vortex system of a formation flight.

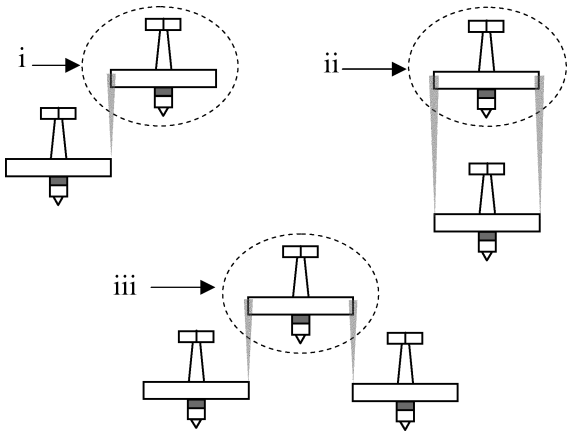

Fig. 2 Types of aircraft formations investigated: i) echelon, ii) lead-trail, and iii) chevron.

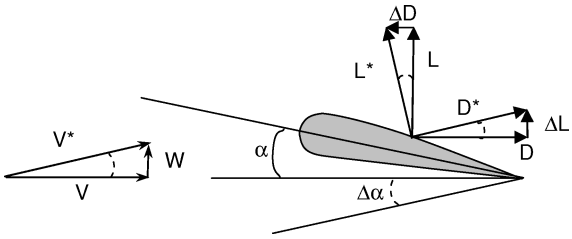

Fig. 3 Small angle changes.

Computations were carried out for three types of formations (Fig. 2). Echelon formation was simulated by using one line vortex interacting with the right wing. Chevron formation and lead-trail formation were simulated by using two line vortices of equal but opposite vorticity interacting with both the right and left wings at equal overlap distance dy from the wing tip, at a vertical spacing z measured from the wing quarter-chord.

It is commonly postulated that the drag reduction is achieved as a result of tilting of the lift vector that occurs while the trailing aircraft is in the upwash of the leading aircraft[2]. The tilted lift and drag vectors are labeled as L^* and D^* in Fig. 3. Thus for a small $\Delta\alpha$ it is assumed that the magnitude of the resultant aerodynamic forces remains approximately constant, or

$$\sqrt{L^2 + D^2} = \sqrt{L^{*2} + D^{*2}} \tag{4}$$

The lift and drag of the trailing aircraft in formation flight are given by

$$L_f = L^*\cos(\Delta\alpha) + D\sin(\Delta\alpha) \tag{5}$$

$$D_f = D^*\cos(\Delta\alpha) - L\sin(\Delta\alpha) \tag{6}$$

The influence of spatial offset is shown in Fig. 4. It can be observed (Fig. 4a) that a negative overlap dy that is, when the vortex core of the leading wing does not impinge on the surface of the trailing wing, results in increase in the lift distribution over the semispan of the trailing wing. For an increasing positive overlap, the lift of the trailing wing experiences a decrease in the outboard region while exhibiting an increase in the inboard region. Figure 4b shows the effect of vertical offset. For the condition of the leading wing vortex core being below $(-z)$ the trailing wing, there is an increase in the lift along the span of the trailing wing. While with the vortex core above the trailing wing $(+z)$ the lift reduces over the span of the trailing wing.

Experimental Setup

Tests were conducted in the Auburn University 3 ft × 4 ft closed-circuit subsonic wind tunnel. A 1:14.5-scale model of the Cessna

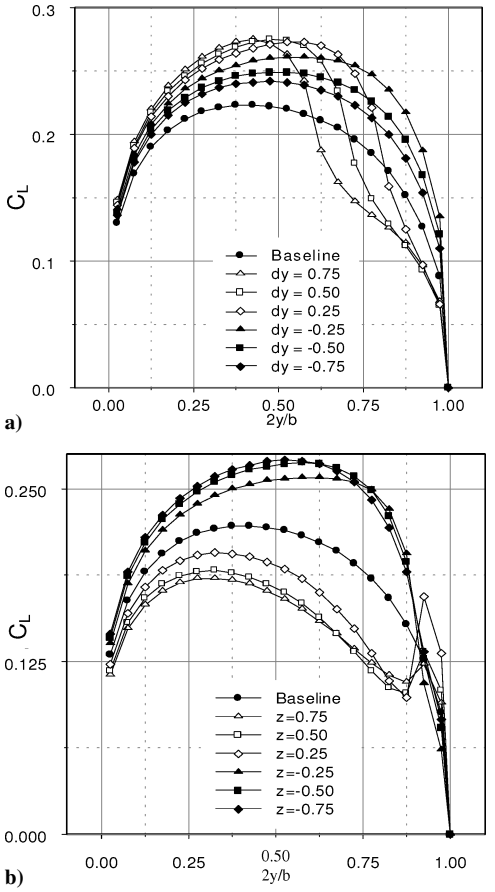

Fig. 4 Spanwise lift distribution of the trailing wing under influence of leading wing for a) $z = 0$ and b) $dy = 0.2$.

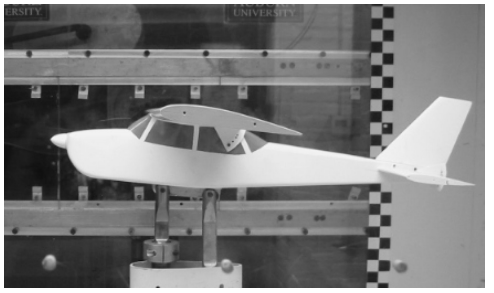

Fig. 5 Cessna model (side view).

172 was used in the tests. Thus the model had a wing span of 30 in. and a chord length of 4.5 in. The model was mounted on an external pyramidal balance at approximately the aerodynamic center (Fig. 5).

The leading aircraft(s) was(were) modeled with the help of semi-infinite wing(s) mounted on adjustable platform(s). These platforms were positioned at a distance of four chord lengths upstream of the trailing aircraft model. The platform(s) provided three degrees of freedom, that is, y, z (Fig. 6), and the angle of attack.

The first configuration tested was the echelon formation. It consisted of a single semi-infinite wing mounted four chords upstream of the test model. The second configuration was for lead-trail flight and consisted of a finite wing mounted directly in front of the aircraft such that it could be adjusted in the z direction, and its angle of attack could be changed. The chevron formation was simulated using two semi-infinite wings mounted on the platforms.

All tests were conducted at a freestream velocity of 110 ft/s. The corresponding Reynolds number was approximately 2.4×10^5. Data were recorded using a National Instruments data-acquisition system in combination with the Labview software. Force and moment data were sampled at 5000 Hz and averaged for every 1-deg increment in angle of attack of the trailing aircraft model.

Results and Discussion

The measured baseline aerodynamic characteristics (C_L and C_D) of the model are compared with Selig's Cessna 172 nonlinear model[11] in Figs. 7 and 8, respectively.

Measurements were then carried out for the three test configurations. Changes in the spanwise location, height, and angle of attack of the leading wing(s) varied trajectory and strength of the trailing vortex and the location of impingement on the trailing aircraft.

Echelon Formation

The resulting variation in forces and moments experienced by the trailing aircraft for the echelon formation is presented in Figs. 9–12. A shift in the C_L vs α as observed. For $z = -0.11$ and $\alpha_{lw} = 10$ deg, the shift was a $\Delta\alpha$ of -4 deg (Fig. 9a), and for $z = 0.33$, $\alpha_{lw} = 6$ deg the shift in $\Delta\alpha$ was -2.5 deg (Fig. 9b), which closely matches the calculated values (Table 1).

For $\alpha < 5$ deg, the $C_{L\alpha}$ is equal to the baseline (0.101/deg). At higher α, the $C_{L\alpha}$ decreases to about 0.066/deg. This is possibly because of the partial stall of the trailing aircraft wing under influence of upwash from the leading wing and vortex interactions.[12] The spanwise location of the trailing aircraft wing where stall initiates

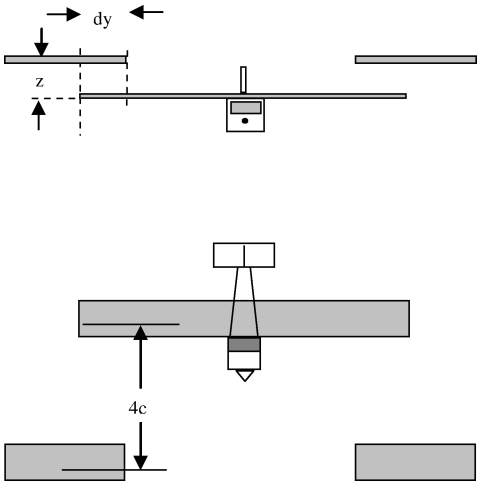

Fig. 6 Front and top view of test setup.

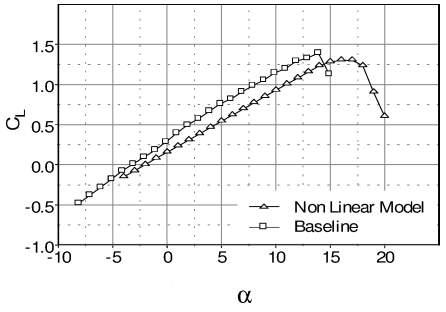

Fig. 7 Comparison of measured C_L to the nonlinear model.

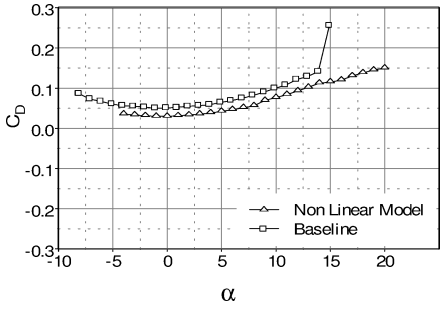

Fig. 8 Comparison of measured C_D to the nonlinear model.

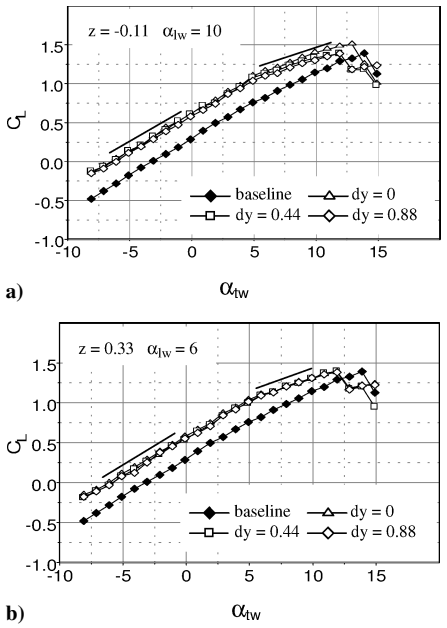

Fig. 9 Lift for echelon configuration.

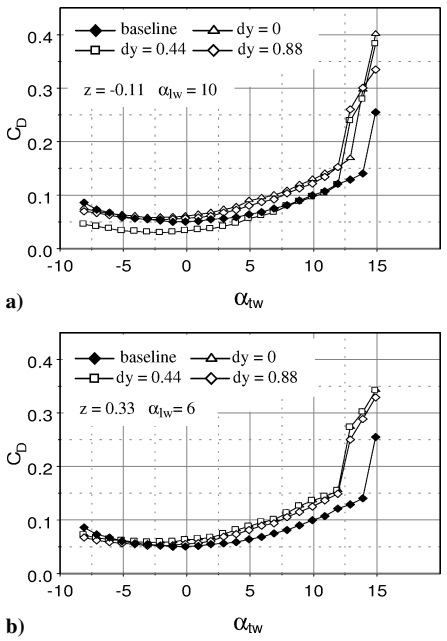

Fig. 10 Drag for echelon configuration.

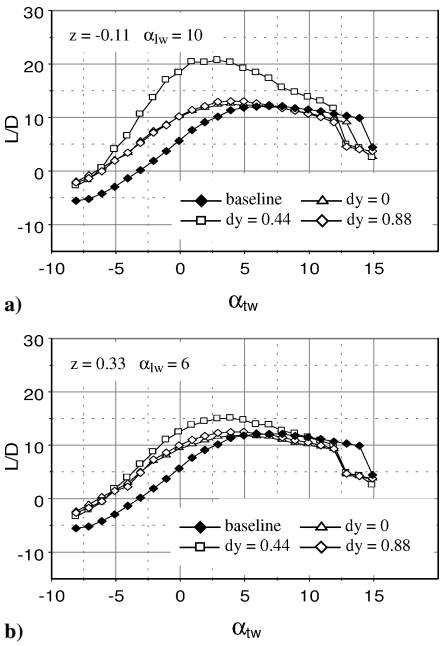

Fig. 11 L/D for echelon configuration.

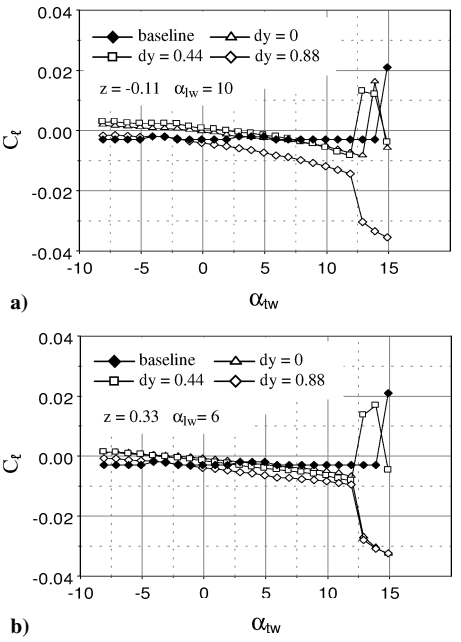

Fig. 12 Rolling moment for echelon configuration.

corresponds to the maximum upwash from the leading wing, thus increasing the overlap results in further reduction of $C_{L\alpha}$. A lower α_{stall} is also observed when the overlap is increased (Fig. 9b).

The drag characteristics are presented in Fig. 10. The drag results show some interesting variations. For both low and high α_{lw}, minimum drag is observed for $dy = 0.44$, which is close to the optimum position for predicted variation in mutual induced drag using the horseshoe-vortex model.[5] The results show higher drag than the baseline data for most of the positive α_{tw}. This indicates that the application of small angle theory to formation flight has its limitations because $\Delta\alpha$ varies significantly over the span, resulting in a spanwise variation in α_{tw}; thus, the experimental values differ from the numerical models based on small angles approximation.[3,4,13] Rapid rise of drag confirms the progression of partial stall on one wing.

The lift-to-drag-ratio (L/D) characteristics are given in Fig. 11. The results indicate a significant increase in L/D for α_{tw} within the standard range of cruise flight. For $z = -0.11$, $\alpha_{\text{lw}} = 10$ deg the L/D increased by about 60%, and for $z = 0.33$, $\alpha_{\text{lw}} = 6$ deg the L/D increases by approximately 25%. Maximum increase in L/D was observed for the case $z = -0.11$ and $dy = 0.44$ matching the various numerical models[3,4,14] and experimental results.[2,6]

The coefficient of rolling moment C is shown in Fig. 12. The C curve shows an inverse correlation with $C_{L\alpha}$ and remains negative for almost the entire range of positive lift.

Lead-Trail Formation

Although lead-trail formation is not observed in migratory birds' flight, it is sometimes necessary to fly lead-trail formation in aircraft, an example being airborne refueling. In this case, the tip vortices of the leading wing are in the same direction as that of trailing aircraft wings. The trailing aircraft is directly in the downwash of the leading wing resulting in a $\Delta\alpha > 0$. In the test configuration the leading wing was of equal span as the trailing aircraft and was positioned and four chord lengths upstream. The $C_{L\alpha}$ plots are shown in Fig. 13 for the two angles-of-attacks cases. The plots indicate a shift in the C_L in

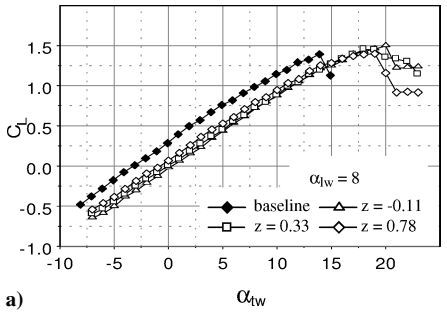

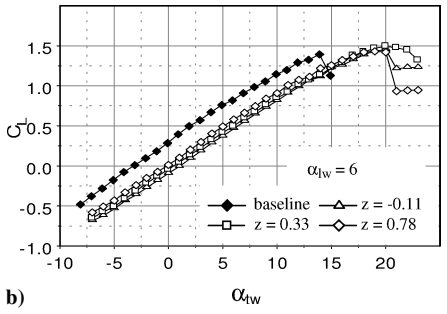

Fig. 13 Lift for lead-trail formation.

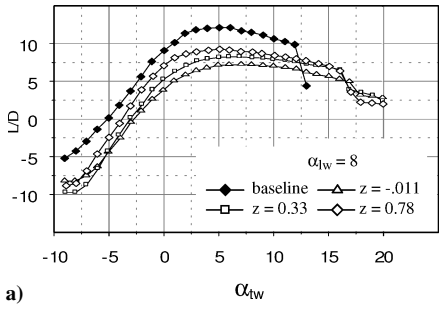

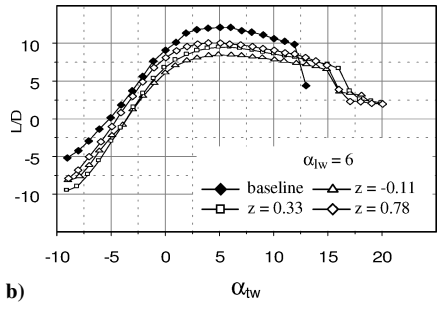

Fig. 14 L/D for lead-trail configuration.

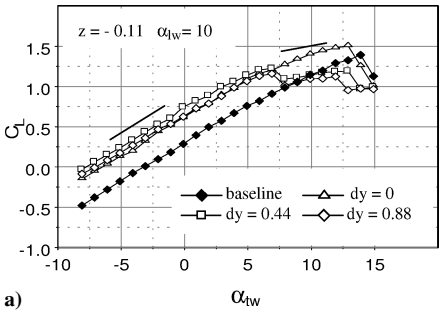

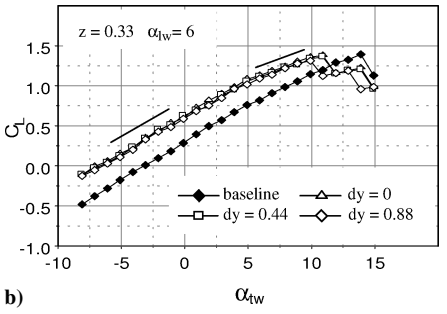

Fig. 15 Lift for chevron configuration.

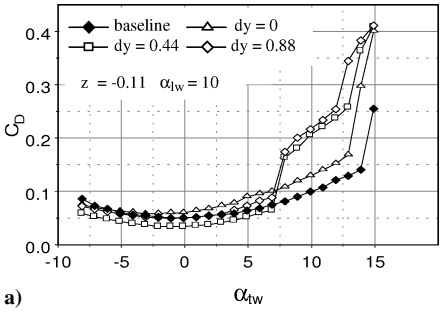

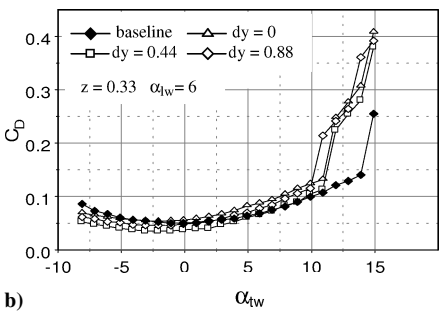

Fig. 16 Drag for chevron configuration.

direction opposite to that of the echelon formation corresponding to $\Delta\alpha$ of approximately 3 deg. A delayed stall, and a higher C_{Lmax}, can also be observed in Fig. 13. This is because of the energizing of the boundary layer on the trailing aircraft wing, which is attributed to the downwash of the leading wing. A reduction in L/D was observed for the entire range of α_{tw} as shown in Fig. 14.

Chevron Formation

In the chevron formation, the port and starboard wings of the trailing aircraft are under the influence of wing-tip vortices from a leading starboard wing and a leading port wing respectively. The C_L vs α_{tw} plots are shown in Fig. 15. It is observed that high upwash and subsequent high $\Delta\alpha$ at the wing tips results in an early stall for the cases where the tip vortices from the leading wings were overlapping the trailing aircraft wings, indicated by $dy > 0$. The shift in C_L has a trend similar to the echelon formation. The average value of $\Delta\alpha = -5$ deg, which is higher in magnitude than the echelon formation. For low α_{tw}, $C_{L\alpha}$ of the trailing aircraft is equal to baseline. At higher α_{tw}, two distinct phenomena are observed depending on α_{lw}. For smaller value of α_{lw}, the slope $C_{L\alpha}$ drops from 0.101/deg to about 0.08/deg. For higher α_{lw}, the value of $C_{L\alpha}$ drops to 0.003/deg. The variation of $C_{L\alpha}$ with dy is approximately twice the value observed in echelon formation. The location of impinging vortex and consequently $\Delta\alpha_{\text{max}}$ plays a significant role in the inception and progression of stall. With an increase in overlap ($dy > 0$), the stall occurs at lower α as the spanwise location, where stall initiates farther from the wing tips. For $\alpha_{\text{lw}} = 8$ deg, a more prominent partial stall is observed for $dy > 0$.

The drag characteristics shown in Fig. 16 clearly indicate the effect of partial stall. It was observed that for the case of high α_{lw} (Fig. 16a) and $dy > 0$, C_D increases significantly at $\alpha_{\text{tw}} = 6$ deg, which corresponds to the stall initiation angle as seen in Fig. 15a. A similar observation can be made for the case of low α_{lw} (Fig. 16b).

An increased L/D is observed for α_{tw} less than the partial stall angle. For the case of $\alpha_{\text{lw}} = 10$ deg, an increase of about 100% was observed (Fig. 17a), whereas a 70% increase in L/D was observed

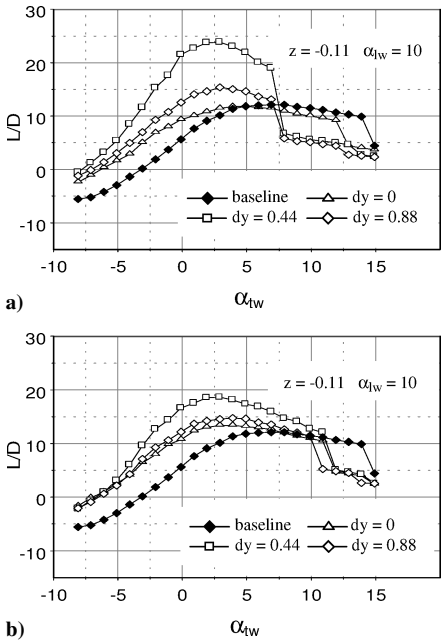

Fig. 17 L/D curves for chevron configuration.

for the low α_{lw}. A sudden drop in L/D is exhibited as a result of the partial stall effects as discussed earlier.

Uncertainty Analysis

The pyramidal balance was calibrated before the testing, and calibration was repeatedly checked using a 5-lb standard benchmark loading for forces and 5 in.-lb for moments. The three force readouts remained within 1.6% of the applied load, and the moment readouts remained within 1.8%. The wind-tunnel speed was measured by a calibrated pressure transducer and cross-checked with a manometer. The average speed accuracy was within 4%. Tunnel temperature and atmospheric pressure were measured within 3% accuracy limits.

Conclusions

A significant increase in L/D was found for both echelon and chevron formations. The lift curve shows three regions for both echelon and chevron formation. At low α_{tw}, the slope $C_{L\alpha}$ is almost equal to the baseline, whereas the curve shifts by $\Delta\alpha$. The value of $\Delta\alpha$ is directly proportional to the circulation of the impinging vortex and therefore α_{lw}. $C_{L\alpha}$ or both echelon and chevron formation was less than the baseline $C_{L\alpha}$ at higher α_{tw}. The drop in $C_{L\alpha}$ shows strong dependence on α_{lw} and the overlap dy. The largest increase in L/D was measured for the chevron formation. The trends in L/D change also indicate an optimal value for the overlap. An undesirable effect of echelon formation is the unbalanced rolling moment experienced by the trailing aircraft. In case of the lead-trail formation, the C_L shift was opposite to other two formations tested. Also, the lead-trail formation exhibited a reduction in the L/D.

References

[1]Gingras, D. R., Player, J. L., and Blake, W. B., "Static and Dynamic Wind Tunnel Testing of Air Vehicles in Close Proximity," AIAA Paper 2001-4137, Aug. 2001.

[2]Ray, R. J., Cobliegh, B. R., Vachon, M. J., and Clinton, St. J., "Flight Test Techniques Used to Evaluate Performance Benefits During Formation Flight," NASA/TP-2002-210730, Aug. 2002.

[3]Iglesias, S., and Mason, W. H., "Optimum Spanloads in Formation Flight," AIAA Paper 2002-0258, Jan. 2002.

[4]Wang, Z., and Mook, D. T., "Numerical Aerodynamic Analysis of Formation Flight," AIAA Paper 2003-610, Jan. 2003.

[5]Blake, W., and Multhopp, D., "Design, Performance and Modeling Considerations for Close Formation Flight," AIAA Paper 98-4343, Aug. 1998.

[6]Vachon, M. J., Ray, R. J., Walsh, K. R., and Ennix, K., " F/A-18 Performance Benefits Measured During Autonomous Formation Flight Project," NASA/TM-2003-210734, Sept. 2003.

[7]Poore, S. O., Sanchez-Haiman, A., and Goslow, G. E., Jr., "Wing Upstroke and the Evolution of Flapping Flight," *Nature*, Vol. 387, June 1997, pp. 799–802.

[8]Dimok, G. A., and Selig, M. S., "The Aerodynamic Benefits of Self-Organization in Bird Flocks," AIAA Paper 2003-0608, Jan. 2003.

[9]Cerretelli, C., and Williamson, C. H. K., "The Physical Mechanism for Merging of Trailing Vortices," AIAA Paper 2003-1287, Jan. 2003.

[10]Miranda, J. A., and Devenport, W. J., "Two Point Measurement in Trailing Vortices," AIAA Paper 96-0804, Jan. 1996.

[11]Roskam, J., "Airplane Flight Dynamics and Automatic Flight Controls, Part I," DARC Corp., Lawrence, KS, 1995.

[12]Leweke, T., and Williamson, C. H. K., "Three Dimensional Dynamics of a Counterrotating Vortex Pair," *Proceedings of the 8th International Symposium on Flow Visualization*, Paper No. 271, Sept. 1998.

[13]Loucel, R. E., and Crouch, J. D., "Flight Simulator Study of Airplane Encounters with Perturbed Trailing Vortices," AIAA Paper 2004-1074, Jan. 2004.

[14]King, R. M., and Gopalarathnam, A., "Ideal Aerodynamics of Ground Effect and Formation Flight," AIAA Paper 2004-0906, Jan. 2004.